A Synchronous Generator Based Diesel-PV Hybrid Micro-grid with Power Quality Controller

Shatakshi, Ikhlaq, *Member, IEEE*, Bhim Singh, *Fellow, IEEE*, and Sukumar Mishra, *Senior Member, IEEE*
Department of Electrical Engineering, Indian Institute of Technology Delhi, New Delhi 110 016, India
Email: shatakshi.b4u@gmail.com, ikhlaqiitd2015@gmail.com, bhimsinghiitd61@gmail.com, sukumariitdelhi@gmail.com

***Abstract*—This paper presents an isolated microgrid, with synchronous generator(SG) based diesel generation(DG) system in combination with solar photo-voltaic(PV). The DG supplies power to the load directly, and a battery supported voltage source converter (VSC) is connected in shunt at point of common coupling (PCC). The PV array is connected at DC-link of the VSC through a boost converter. A high order optimization based adaptive filter control scheme is used for maintaining the quality of PCC voltages and source currents. This controller makes the waveform free of distortion, removes errors due to unbalances, corrects the power factor and makes the source current smooth sinusoidal, irrespective of the nature of load. MATLAB/Simulink based simulation results demonstrate satisfactory performance of the given system.**

***Index Terms*—Battery, diesel generator, LMF, power quality, PV.**

I. Introduction

BURNING of fossil fuels for producing electricity has been a major cause of global warming [1]. Thus, researchers have been looking for alternative sources for electricity production, which are sustainable and environment friendly [2]. Moreover, countries are working towards making their whole automobile fleet and electricity production sectors free of burning fossil fuels [3]. This has led to rise in renewable based energy systems such as PV, wind, hydro, biomass, ocean thermal energy, tidal energy, etc. Lately, renewable energy based microgrids are becoming increasingly popular to supply power to urban, rural or remote areas. Such systems can be operated with or without grid [4]. These sources are imperishable and cause no harm to the environment, however, their variable and fluctuating nature makes the task of integrating them a real challenge [5]. This gives rise to the need of intelligent controllers which can regulate the voltage, current and frequency of the system in case of presence/absence of grid or linear/nonlinear load or unbalance in the three-phase systems, and hence, make the system more stable, reliable and secure.

Diesel engines can be used with permanent magnet synchronous generators, induction generators or synchronous reluctance generators, etc. [6], [7]. The best fuel efficiency is obtained in diesel generators when they are operated at 80% to 100% of their rated capacity [8]. Diesel generators have been source of electricity for long. In urban areas, they are used as a back-up where as in rural areas, it is one of the primary sources of electricity. Thus, the PV based microgrids could be made more stable and reliable by integrating them with diesel generators. Many authors have worked on such systems and proposed controllers for regulating voltage, current and power flow [9], [10]. However, use of energy storage devices along with PV-DG not only helps in reducing rating of DG, it also efficiently takes care of the transients and maintains the DC-link voltage [11].

Many researchers have proposed power quality controllers for micro-grids. Least mean square (LMS) is an old technique of removing noise and distortions from the signal. Based on LMS, algorithms such as hyperbolic tangent function based LMS [12], modified variable step filtered-x LMS (FXLMS) based control [13], etc. have been presented in order to achieve load leveling, voltage and frequency control and power quality enhancement. LMF is a higher order filter as compared to LMS, and thus, it has a higher signal to noise ratio (SNR) [14]. The superiority of this control over conventional LMS algorithms, in terms of mean square error (MSE) and stability, has been presented in [15] and [16].

This paper demonstrates an adaptive filter, in a three-phase DG-PV based isolated micro-grid. It removes the harmonics present in the current due to the nonlinear loads, and makes it smooth sinusoidal, thus, reducing the total harmonic distortion (THD) as per IEEE-519 standard. A boost converter connects PV and DC-link of VSC, and executes the maximum power point tracking (MPPT) for PV array. The battery is directly connected at the DC-link.

The paper is organized as follows. The system design and modeling are presented in section II. Section III describes control scheme. In section IV, the simulated results for different scenarios have been discussed. Section V concludes the paper.

II. System Design and Modeling

Fig. 1 depicts the configuration of the system. A two stage PV system is supplying power to the nonlinear load, through a VSC. The battery is connected directly at the DC-link. An SG based DG is connected at PCC to provide support power in case of low or absence of insolation. The components of the system are designed as follows.

A. Source and Load Design

For supplying power to the nonlinear load varying between 10kW to 15kW, a SG of $10kW, 415V, 50Hz$ is taken to be coupled to a diesel engine. The PV array can be designed to give maximum power of 10kW so that both sources alone are

978-1-5090-1412-5/17/$31.00 ©2017 IEEE

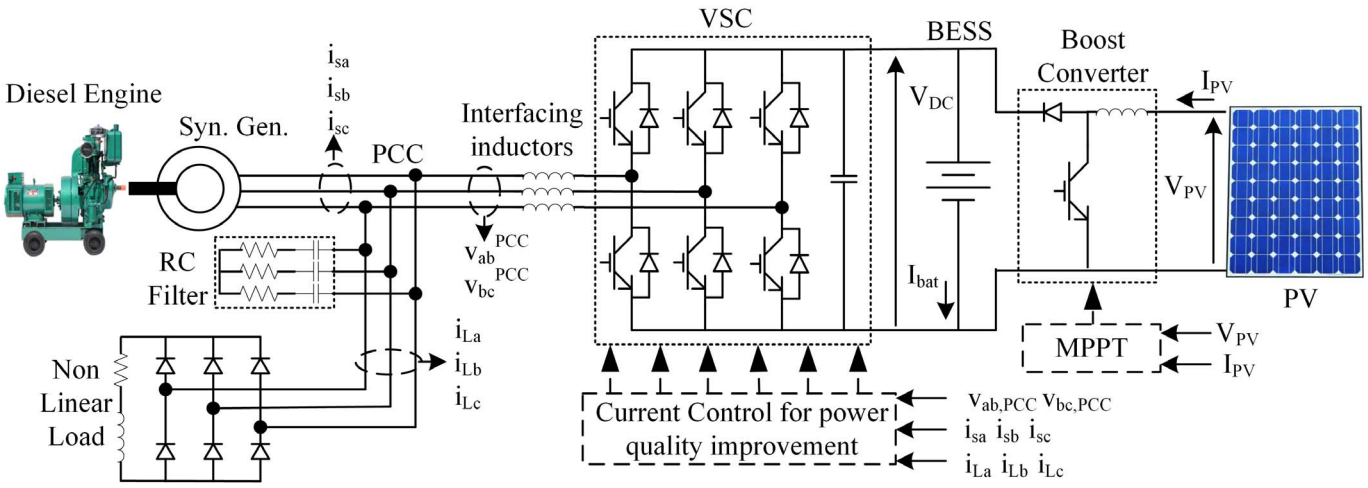

Fig. 1 System model

also able to support bare minimum load. The number of series and parallel modules to be connected can be calculated as,

$$n_s = \frac{V_{DC}}{V_{oc}} = \frac{700}{36} \approx 20 \text{ modules} \tag{1}$$

$$n_p = \frac{P_{max}/V_{DC}}{I_{mp}} = \frac{10,000/700}{7.35} \approx 2 \text{ modules} \tag{2}$$

where V_{oc}, I_{mp} and P_{max} represent the open circuit voltage, peak current and maximum power given by PV.

B. Boost Converter Design

DC-DC boost converter is used to operate PV array at MPPT at all times. Simple and effective P&O MPPT technique is used which perturbs the the duty ratio continuously in order to track the maximum power point [17]. The value of inductor needs to be designed based on the PV rating and DC-link voltage as,

$$L_{boost}^{mppt} = \frac{(V_{out} - V_{in})(V_{in}/V_{out})}{\Delta I_{PV} \times freq} \tag{3}$$

$$L_{boost}^{mppt} = \frac{(700 - 580)(580/700)}{5.88 \times 10,000} = 1.7 \approx 2mH \tag{4}$$

where $freq$ represents the switching frequency, ΔI_{PV} is the ripple present in PV current.

C. DC-link Design

The DC link voltage level depends on the level of AC side voltage as,

$$V_{DC} = \frac{2\sqrt{2}V_{LL}}{\sqrt{3}m} = \frac{2\sqrt{2} \times 415}{\sqrt{3} \times 1} \approx 700V \tag{5}$$

where V_{LL} is the AC side line voltage and m is the modulation index. A capacitor is also placed at the DC-link to absorb the transients. The value of capacitor for 2% ripple in DC-link voltage can be determined as,

$$C_{DC} = \frac{P_{DC}/V_{DC}}{2\omega \times V_{DC}^{rip}} = \frac{10,000/700}{2 \times 314 \times 14} \approx 2mF \tag{6}$$

A battery of 700V is chosen to be directly connected on DC link. The Ah rating of battery is taken as 50Ah to provide losses and suppress the PV power fluctuations.

D. Inductive and Capacitive Filters for VSC

To compensate the current and voltage ripples, inductive and capacitive filters are connected in series and shunt of VSC respectively. The inductor values can be estimated as,

$$L_f = \frac{\sqrt{3} \times m \times V_{DC}}{12 \times h \times freq \times \Delta I} \approx 2mH \tag{7}$$

where h is the overloading factor, taken as 1.2. ΔI is the current ripple, chosen as 3% of the VSC current. An inductor of 2mH is placed in each phase.

The capacitive filters should be designed in such a way that they offer low impedance at high frequencies and high impedance at fundamental frequencies. For a 5Ω resistance and $5\mu F$ capacitance, an impedance of 6.36Ω is offered to frequency of 5kHz and at fundamental frequency, it is 636Ω. Thus, these values are used for the shunt filter.

III. VSC Control

The adaptive control for regulating power quality at PCC through VSC is shown in Fig. 2. It calculates the weight of the active and reactive components of currents and estimates the reference current for each phase, using the in-phase and quadrature unit templates of voltage.

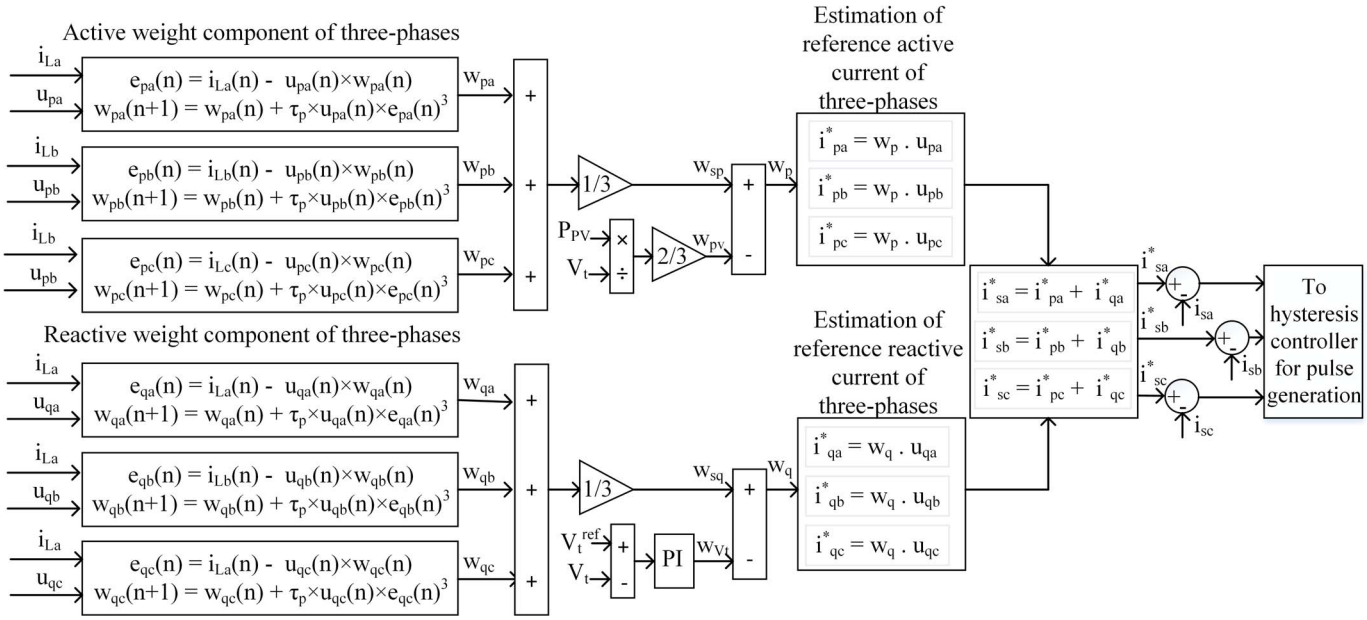

Fig. 2 Adaptive filter for power quality improvement

A. Generating Unit Templates

As only line voltages are sensed to reduce the number of sensors from three to two, phase voltages are estimated as,

$$\begin{cases} v_{sa} &= \frac{2v_{sab}+v_{sbc}}{3} \\ v_{sb} &= \frac{-v_{sab}+v_{sbc}}{3} \\ v_{sc} &= \frac{-v_{sab}-2v_{sbc}}{3} \end{cases} \tag{8}$$

Thus, the terminal voltage V_t would be,

$$V_t = \sqrt{\frac{2}{3}(v_{sa}^2 + v_{sb}^2 + v_{sc}^2} \tag{9}$$

The in-phase and quadrature voltage templates are calculated using V_t as,

$$u_{ap} = \frac{v_{sa}}{V_t};\ u_{bp} = \frac{v_{sa}}{V_t};\ u_{cp} = \frac{v_{sa}}{V_t} \tag{10}$$

$$\begin{cases} u_{aq} = -\frac{u_bp}{\sqrt{3}} + \frac{u_{cp}}{\sqrt{3}} \\ u_{bq} = \frac{\sqrt{3}u_ap}{2} + \frac{(u_{bp}-u_{cp})}{2\sqrt{3}} \\ u_{cq} = -\frac{\sqrt{3}u_ap}{2} + \frac{(u_{bp}-u_{cp})}{2\sqrt{3}} \end{cases} \tag{11}$$

B. Generating the Weight Components

The weight of load component for each phase at a particular instant is estimated based on the weight and error at previous instant. Thus, the weights adjust themselves automatically, making the control adaptive.

First the error is defined based on the load current and calculated reference current as,

$$e_{pa}(n) = i_{La}(n) - u_{pa} \times w_{pa}(n) \tag{12}$$

where $w_{pa}(n)$ is the weight component for fundamental active component of phase-a. The weight is updated using the active adaptation constant $\tau_p = 0.0002$ as,

$$w_{pa}(n+1) = w_{pa}(n) + \tau_p \times u_{pa}(n) \times (e_{pa}(n))^3 \tag{13}$$

Correspondingly, the errors and active weight components for phase-b and phase-c can be determined as,

$$\begin{aligned} e_{pb}(n) &= i_{Lb}(n) - u_{pb} \times w_{pb}(n) \\ w_{pb}(n+1) &= w_{pb}(n) + \tau_p \times u_{pb}(n) \times (e_{pb}(n))^3 \end{aligned} \tag{14}$$

$$\begin{aligned} e_{pc}(n) &= i_{Lc}(n) - u_{pc} \times w_{pc}(n) \\ w_{pc}(n+1) &= w_{pc}(n) + \tau_p \times u_{pc}(n) \times (e_{pc}(n))^3 \end{aligned} \tag{15}$$

Similarly, the error for the reactive component of current of phase-a is calculated using load current and reference current as,

$$e_{qa}(n) = i_{La}(n) - u_{qa} \times w_{qa}(n) \tag{16}$$

Thus, the weights of reactive components are updated for phase-a based on the reactive adaptation constant $\tau_q = 0.0002$ and unit template u_{qa} as,

$$w_{qa}(n+1) = w_{qa}(n) + \tau_{qa} \times u_{qa}(n) \times (e_{qa}(n))^3 \tag{17}$$

where e_{qa} is the error, and w_{qa} is the reactive weight component for phase-a. Thus, weights for phase-b and phase-c can be determined on similar lines as,

$$\begin{aligned} e_{qb}(n) &= i_{Lb}(n) - u_{qb} \times w_{qb}(n) \\ w_{qb}(n+1) &= w_{qb}(n) + \tau_q \times u_{qb}(n) \times (e_{qb}(n))^3 \end{aligned} \tag{18}$$

$$\begin{aligned} e_{qc}(n) &= i_{Lc}(n) - u_{qc} \times w_{qc}(n) \\ w_{qc}(n+1) &= w_{qc}(n) + \tau_q \times u_{qc}(n) \times (e_{qc}(n))^3 \end{aligned} \tag{19}$$

C. Generating Reference Currents

After calculating the active and reactive weights of all the phases separately, the total active component w_{sp} is determined by the average of all components as,

$$w_{sp} = \frac{w_{pa} + w_{pb} + w_{pc}}{3} \tag{20}$$

The net active component for calculating reference signal would be determined by subtracting the PV component from total weight. Thus, the active reference current component for each phase can be found using the net active component and the respective in-phase unit template as,

$$\begin{cases} i^*_{pa} = (w_{sp} - w_{pv}) \cdot u_{pa} \\ i^*_{pb} = (w_{sp} - w_{pv}) \cdot u_{pb} \\ i^*_{pc} = (w_{sp} - w_{pv}) \cdot u_{pc} \end{cases} \tag{21}$$

The total reactive component of each phase is calculated as,

$$w_{sq} = \frac{w_{qa} + w_{qb} + w_{qc}}{3} \tag{22}$$

This is used to find the reactive component of the reference of each phase, after subtracting the terminal voltage weight, using the respective quadrature unit templates as,

$$\begin{cases} i^*_{qa} = (w_{sq} - w_{vt}) \cdot u_{qa} \\ i^*_{qb} = (w_{sq} - w_{vt}) \cdot u_{qb} \\ i^*_{qc} = (w_{sq} - w_{vt}) \cdot u_{qc} \end{cases} \tag{23}$$

Once the active and reactive components of each phase are obtained, the net reference current for each phase is calculated as,

$$i^*_{sa} = i^*_{pa} + i^*_{qa};\ i^*_{sb} = i^*_{pb} + i^*_{qb};\ i^*_{sc} = i^*_{pc} + i^*_{qc} \tag{24}$$

These are compared with the actual senses phase currents i_{sa}, i_{sb}, i_{sc}. The error is passed through the hysteresis controller, which gives fast response in transients, in order to generate the gating pulses for VSC.

IV. Simulation Results

The proposde micro-grid is simulated in MATLAB/Simulink and the responses for change in load, load unbalance and PV variation are observed.

A. Steady State Operation

The steady state response where the load is constant, and is supplied power by both DG and PV, is shown in Fig. 3. The DC side parameters i.e. PV voltage, current and power, DC-link voltage and battery current can be seen in Fig. 3(a). It can be noted that PV is operating in MPPT at solar insolation of $500W/m^2$. The load and DG side voltage and currents are shown in Fig. 3(b). The internal parameters of the control w_p and e_{pa} are also shown in the same figure. The THD in currents and voltage are presented in Table I.

B. Effect of PV variation

The response of system to PV insolation change is depicted in Figs. 4(a) and (b). At $t = 1s$, insolation rises from $500W/m^2$ to $1000W/m^2$, raising the PV power from $4.2kW$ to $8.4kW$ approximately, as seen in Fig. 4(a). Since the load current is constant, this leads to decrease in the net active weight of the DG current, thus, reducing the current drawn from DG. The same is depicted in Fig. 4(b). The DC-link and AC voltages are maintained constant by battery and VSC.

C. Effect of Demand Variation

The effect of change in load is demonstrated in Figs. 4(c) and (d). The DC side voltage current and power remain same, as their is no change in the solar insolation. It can be observed from Fig. 4(d), that the reduction in load simply lowers down the current drawn from DG, as the active weight component has been decreased by the VSC controller. The quality of current and voltage are regulated all the time.

D. Effect of Unbalance

A single-phase open circuit fault is created in phase-a. The response of system is shown in Figs. 4(e) and (f). As net load has reduced, the source current of each phase is reduced, but it is still maintained balanced and pure sinusoidal by the controller. The system smoothly recovers and quickly reaches normal steady state, with normal DC and AC voltages.

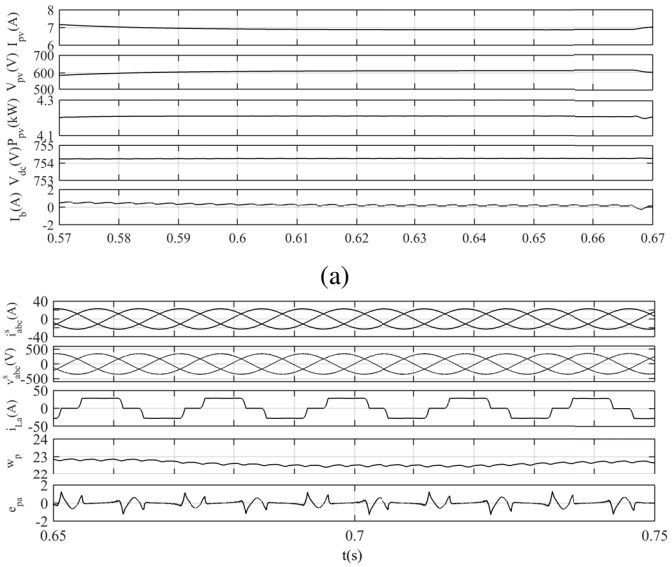

Fig. 3 Steady State Response of DG-PV micro-grid

TABLE I
TOTAL HARMONIC DISTORTIONS

Parameter	Signal	THD
Load Current	i_{La}	26.69%
DG Current	i_{sa}	2.05%
PCC Voltage	v_{sab}	3.67%

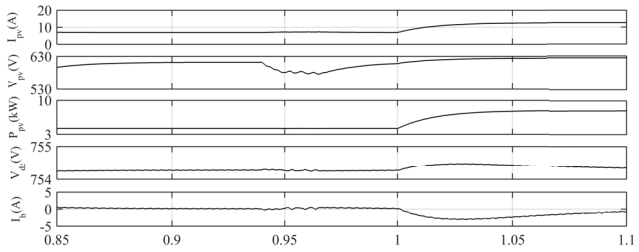

(a)

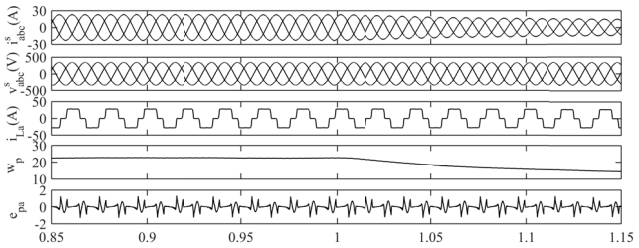

(b)

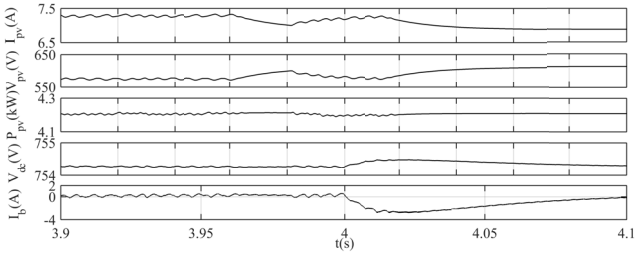

(c)

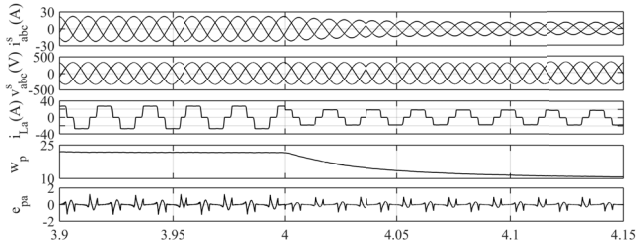

(d)

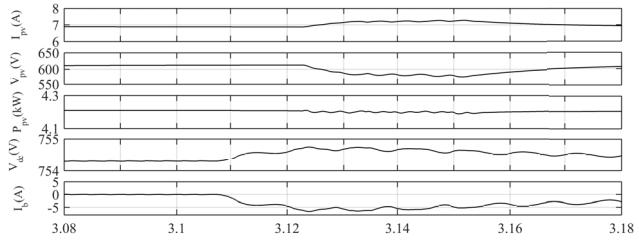

(e)

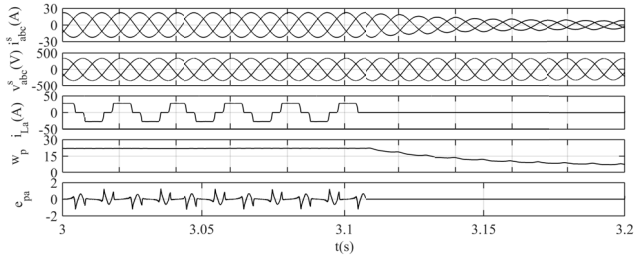

(f)

Fig. 4 Dynamic Response of DG-PV micro-grid

V. Conclusion

An isolated SG based DG and PV hybrid micro-grid has been presented here, with a battery suppported VSC connected at PCC. Three-phase adaptive control is used for power quality improvement through VSC. The given system and control have been simulated in MATLAB/Simulink environment and results demonstrate their satisfactory performance in both steady state and dynamic conditions.

Acknowledgement

This work was supported in part by DST, Govt. of India under Grant Number RP02979 (Project RESCUES).

References

[1] G. Shafiullah et al., "Meeting energy demand and global warming by integrating renewable energy into the grid," in *22nd Australasian Universities Power Engg. Conf. (AUPEC)*, pp. 1–7, Bali, 2012.

[2] M. Milligan et al., "Alternatives No More: Wind and Solar Power Are Mainstays of a Clean, Reliable, Affordable Grid," *IEEE Power & Energy Mag.*, vol. 13, no. 6, pp. 78–87, Nov.-Dec. 2015.

[3] L. Partain and L. Fraas, "Displacing California's coal and nuclear generation with solar PV and wind by 2022 using vehicle-to-grid energy storage," *IEEE Photovoltaic Specialist Conf.*, pp. 1–6, LA, 2015.

[4] Daniel E. Olivares et al., "Trends in Microgrid Control," in *2015 IEEE Trans. Smart Grid*, vol. 5, no.4, pp. 1905–1919, July, 2014.

[5] Z. Zavody, "The grid challenges for renewable energy An overview and some priorities," *IET Seminar on Integrating Renewable Energy to the Grid*, pp. 1–24, London 2014.

[6] G. Pathak, B. Singh and B. K. Panigrahi, "Permanent magnet synchronous generator based wind energy and DG hybrid system," *IEEE Nat. Power Systems Conf. (NPSC)*, pp. 1–6, Guwahati, 2014.

[7] G. Pathak, B. Singh and B. K. Panigrahi, "Isolated microgrid employing PMBLDCG for wind power generation and synchronous reluctance generator for DG system," *IEEE 6th India Int. Conf. Power Electron. (IICPE)*, pp. 1–6, Kurukshetra,2014.

[8] P. J. Chauhan et al., "Fuel efficiency improvement by optimal scheduling of diesel generators using PSO in offshore support vessel with DC power system architecture," *IEEE PES Asia-Pacific Power & Energy Engg. Conf. (APPEEC)*, Brisbane, QLD, 2015, pp. 1-6.

[9] S. Mishra, D. Ramasubramanian and P. C. Sekhar, "A Seamless Control Methodology for a Grid Connected and Isolated PV-Diesel Microgrid," *IEEE Trans. Power Syst.*, vol. 28, no. 4, pp. 4393-4404, Nov. 2013.

[10] M. Datta, T. Senjyu, A. Yona, T. Funabashi and C. H. Kim, "A Coordinated Control Method for Leveling PV Output Power Fluctuations of PVDiesel Hybrid Systems Connected to Isolated Power Utility," *IEEE Trans. Energy Convers.*, vol. 24, no. 1, pp. 153-162, March 2009.

[11] R. W. Wies, R. A. Johnson, A. N. Agrawal and T. J. Chubb, "Simulink model for economic analysis and environmental impacts of a PV with diesel-battery system for remote villages," *IEEE Trans. Power Syst.*, vol. 20, no. 2, pp. 692-700, May 2005.

[12] B. Singh, R. Niwas and S. K. Dube, "Load Leveling and Voltage Control of Permanent Magnet Synchronous Generator-Based DG Set for Standalone Supply System," *IEEE Trans. Ind. Informat.*, vol. 10, no. 4, pp. 2034-2043, 2014.

[13] R. Niwas and B. Singh, "Solid-state control for reactive power compensation and power quality improvement of wound field synchronous generator-based diesel generator sets," *IET Electric Power App.*, vol. 9, no. 6, pp. 397-404, 2015.

[14] R. K. Agarwal, I. Hussain and B. Singh, "LMF-Based Control Algorithm for Single Stage Three-Phase Grid Integrated Solar PV System," *IEEE Trans. Sust. Energy*, vol. 7, no. 4, pp. 1379-1387, Oct. 2016.

[15] J. C. M. Bermudez and V. H. Nascimento, "When is the least-mean fourth algorithm mean-square stable?," *Proc. IEEE Int. Conf. Acoust. Speech Sig. Process.*, vol. 4, pp. iv/341-iv/344, Mar. 18-23, 2005.

[16] E. Eweda, "Global stabilization of the least mean fourth algorithm," *IEEE Trans. Sig. Process.*, vol. 60, no. 3, pp. 1473-1477, Mar. 2012.

[17] O. Ibrahim, N. Z. Yahaya, N. Saad and M. W. Umar, "Matlab/Simulink model of solar PV array with perturb and observe MPPT for maximising PV array efficiency," *IEEE Conf. Energy Conver. (CENCON)*, pp. 254-258, 2015.